

Article

Integrating Spatial Continuous Wavelet Transform and Normalized Difference Vegetation Index to Map the Agro-Pastoral Transitional Zone in Northern China

Yinan Han ^{1,*}, Jian Peng ^{1,*}, Jeroen Meersmans ² , Yanxu Liu ³, Zhiqiang Zhao ⁴ and Qi Mao ¹

¹ Laboratory for Earth Surface Processes, Ministry of Education, College of Urban and Environmental Sciences, Peking University, Beijing 100871, China; helenhyn1989@163.com (Y.H.); maoqi@pku.edu.cn (Q.M.)

² School of Water, Energy and Environment, Cranfield University, Bedfordshire MK43 0AL, UK; jeroen.meersmans@cranfield.ac.uk

³ State Key Laboratory of Earth Surface Processes and Resource Ecology, Faculty of Geographical Science, Beijing Normal University, Beijing 100875, China; yanxuliubnu.edu.cn

⁴ Center for Systems Integration and Sustainability, Department of Fisheries and Wildlife, Michigan State University, East Lansing, MI 48824, USA; zqzhao0324@gmail.com

* Correspondence: jianpeng@urban.pku.edu.cn; Tel.: +86-010-6275-0926

Received: 29 October 2018; Accepted: 28 November 2018; Published: 30 November 2018



Abstract: The agro-pastoral transitional zone (APTZ) in Northern China is one of the most important ecological barriers of the world. The commonly-used method to identify the spatial distribution of ATPZ is to apply a threshold rule on climatic or land use indicators. This approach is highly subjective, and the quantity standards vary among the studies. In this study, we adopted the spatial continuous wavelet transform (SCWT) technique to detect the spatial fluctuation in normalized difference vegetation index (NDVI) sequences, and as such identify the APTZ. To carry out this analysis, the Moderate Resolution Imaging Spectroradiometer (MODIS) NDVI 1-month data (MODND1M) covering the period 2006–2015 were used. Based on the spatial variation in NDVI, we identified two sub-regions within the APTZ. The temporal change of APTZ showed that although vegetation spatial pattern changed annually, certain areas appeared to be stable, while others showed higher sensitivity to environmental variance. Through correlation analysis between the dynamics of APTZ and precipitation, we found that the mean center of the APTZ moved toward the southeast during dry years and toward the northwest during humid years. By comparing the APTZ spatial pattern obtained in the present study with the outcome following the traditional approach based on mean annual precipitation data, it can be concluded that our study provides a reliable basis to advance the methodological framework to identify accurately transitional zones. The identification framework is of high importance to support decision-making in land use management in Northern China as well as other similar regions around the world.

Keywords: ecological boundary; spatial identification; temporal change; agro-pastoral transitional zone

1. Introduction

An ecological boundary is defined as a complex zone between two contrasting habitat patches [1]. According to different situations, such a boundary could be either narrow or wide, distinct or subtle [2]. The landscape within and nearby an ecological boundary presents a remarkable discontinuity compared with the surrounding areas, which embody both landscape features and structures.

This discontinuity is caused by large scale changes in environmental factors, which are a range of significant exogenous forces with either natural or anthropogenic characteristics [3]. Under the current influences of climate change and human disturbance, the ecosystems in an ecological boundary are more sensitive than those in the surrounding areas because the adaptation of species within these areas may be at their limit and the species may respond gravely when subjected to environmental change [4]. Therefore, an ecological boundary is known as an important object in ecological research, planning and management. Detecting the location of an ecological boundary and characterizing its spatial pattern provide an important basis for the further researches [5].

One way to classify ecological boundaries is to measure the changes in environmental variables and response variables [3]. Environmental variables are exogenous forces such as climate, human activities, landform and soil conditions. Changes in environmental variables cause changes in response variables, which are endogenous factors including biological diversity, population of specific species, vegetation and landscape [3]. One type of ecological boundary is caused by steep gradients of exogenous forces, and can be easily identified by measuring changes in environmental variables. However, another type of ecological boundary may be the result of a much more gradual change in environmental variables that lead to a subtle or drastic change in response variables [2,3,6]. Because of its greater complexity, researchers have paid more attention to find effective ways to detect the latter type of ecological boundary. The agro-pastoral transitional zone (APTZ) in Northern China is one of the world's largest ecological boundaries that belongs to this category [7]. The APTZ links China's agricultural region in the southeast with pastoral region in the northwest, and functions as a natural ecological shelterbelt and agricultural productivity supplier for Northern China. Encompassing both semi-humid and semi-arid areas, the vegetation in this region showed nonlinear dynamics and complex spatial patterns [8,9] and is continuously threatened by climate change, population growth and economic development [10–12]. These influences make the APTZ a highly dynamic area facing multiple environmental issues, such as land overuse, vegetation destruction and ecological degradation [13,14].

To better preserve the function of the ecosystems and sustainably use the land resources, it is important to identify and characterize the APTZ objectively and precisely. Finding an efficient detector that can accomplish these goals is often the main research objective in related studies. An optimal way to identify ecological boundaries is to measure the highest rate of change in response variables [15,16]. Among such variables, the density of specific species is the most representative one. For example, Fortin [16] quantified all 35 species from a hardwood forest in New York within an area of 60 m × 140 m in order to locate the ecological boundary using a lattice-wombling edge detection algorithm. However, species density data requires a large number of field work that is difficult and costly to make and update [3,16,17]. As a result, vegetation is commonly used as a valid proxy, because it can be easily quantified and conveniently spatialized using remote sensing data [16].

Additionally, mathematical techniques have been developed to analyze the features of response variables. Spatial clustering, for example, is a useful method in detecting distinct boundaries; however, they are not so suitable for detecting gradient boundaries [18,19]. Focusing on the gradient boundaries, kernel detectors, such as lattice wombling and the Laplacian kernel, have been applied to identify changes in response variables. However, kernel detectors are too sensitive to local noise and are easily influenced by the fluctuation of adjacent elements at small scales [3]. In contrast, the wavelet transform is a hierarchical method that is relatively less sensitive to local noise, and has been proven to be a successful method when analyzing complex and nonstationary patterns [20]. Wavelet transforms have been widely used to detect the edge of images [21] and to analyze the pattern of temporal signals [22]. Moreover, the wavelet transform is an efficient detector for identifying ecological boundaries [23,24].

Although previous studies have put much effort into identifying the spatial coverage of the APTZ and its change over time, some issues remain open to discussion. Firstly, the frequently used indicators to delineate the APTZ are climate factors and land use factors, such as mean annual precipitation, inter-annual precipitation variability, humidity index and arid index, and the spatial

distribution of cultivated land, grassland and forest [25]. Response variables, especially vegetation factors, have been used rarely. The argument over indicator selection and threshold determination has not been settled [10,25]; therefore, a conclusive and widely acknowledged definition of the APTZ distribution is still not available. Furthermore, many studies concerning APTZ dynamics commonly focused on the dynamics in climate, vegetation, land use, ecosystem services and productivity within a certain area, with the assumption that the location of the APTZ is stable over the timescale of a few decades [9,11,13,26–29]. The temporal changes of APTZ spatial coverage still need further investigation. For example, Li et al. [30] applied wavelet transform to analyze the mutation points of APTZ using a normalized difference vegetation index (NDVI) and precipitation data in one single year, and Zhao [31] made a progress in long term analysis by mapping occurrence frequency of mutation points and discussed relations between the temporal change of mutation points and climatic factors around selected meteorological stations. However, since APTZ is a wide boundary that covers over 500,000 km² [25], the mutation points of NDVI and climatic factors were not sufficient to delineate its coverage. Although there are some studies focusing on the APTZ response to climate change and land use change [10,25,32], the dynamic analysis of APTZ based on response variables and spatial disparity and sub-regions within the APTZ have not drawn much attention.

Broadly adapting from Li et al. [30] and Zhao [31], this study aimed to develop an improved technique for identifying APTZ in Northern China. The specific objectives were: (i) to map the average state and spatial disparity of the APTZ for the period 2006–2015; (ii) to uncover how the spatial disparity changed annually during 2006–2015; and (iii) to analyze the movement of the center of the APTZ and its correlation with annual precipitation during 2006–2015. NDVI, one of the most useful indexes for characterizing vegetation coverage and density [33], was used as the response variable to spatially identify the APTZ, together with the methods of spatial continuous wavelet transform (SCWT) and kernel density estimation.

2. Materials and Methods

2.1. Study Area, Data Sources and Sampling

The APTZ is located in Northern China. The southeast side of the APTZ, known as the North China Plain, has a history of crop farming going back thousands of years and is currently still primarily used for agricultural production. The northwest side of the APTZ is the traditional grazing region and is covered mainly by grassland, shrubland and desert [13]. Crop and livestock farming within the APTZ are distributed discontinuously. Determined by climate, landform and human activities, the APTZ extends from the southern part of the Greater Hinggan Range towards the southwest and reaches the edge of the Qinghai-Tibet Plateau. The 400 mm isohyet is the approximate center line of the APTZ [25]. The study area considered in this research has a surface of 503,100 km² and includes the area from the western part of Jilin and Liaoning Provinces, the southern part of Inner Mongolia Autonomous Region and the northern part of the Hebei, Shanxi and Shaanxi province (Figure 1). This study area follows the trend of the 400 mm isohyet. To establish sample locations for the indicator value, the FISHNET Tool in ArcGIS software (V10.2, ESRI, Inc., Redlands, CA, USA) was used to construct 130 parallel lines over the study area, spaced 10 km apart. Each line contains 40 sample points, also at intervals of 10 km. The sampling lines were perpendicular to the trend of the 400 mm isohyet, giving them an approximately southeast-northwest orientation.

NDVI was used as the indicator to detect the spatial characteristic of the APTZ, and annual precipitation was used as the climate factor. NDVI data have significant advantages in terms of accessibility, updating and accuracy, and therefore, provide a continuous temporal data sequence for dynamic analysis. In this study, we focused on the characteristics of the APTZ over the most recent decade (2006–2015). In order to carry out this analysis in an effective way, the Moderate Resolution Imaging Spectroradiometer (MODIS) NDVI 1-month (MODND1M) data for 2006–2015 were used. These data have a spatial resolution of 500 m × 500 m, and were provided by International Scientific

and Technical Data Mirror Site, Computer Network Information Center of the Chinese Academy of Sciences (<http://www.gscloud.cn>). To better describe the heterogeneity of vegetation growth in semi-humid and semi-arid study areas, and to avoid data variations caused by cloud cover and other uncertain factors, the maximum value of each cell in the summer season (June to August) was used to represent the vegetation condition of each year [34]. Furthermore, for each cell, the mean NDVI value within a neighborhood with a radius 5 km was calculated in order to reduce the local noise of fragmented patches, such as water bodies and artificial surfaces.

The annual precipitation data were provided by the China National Meteorological Data Service Center (<http://data.cma.cn>), which were calculated from the monthly surface climate grid data with a resolution of $0.5^\circ \times 0.5^\circ$. Based on the annual precipitation data, the anomalies in the total precipitation were determined for each year, and used to classify the studied period into relatively dry years and relatively humid years. All data analyses and manipulations were carried out using the ArcGIS 10.2 software.

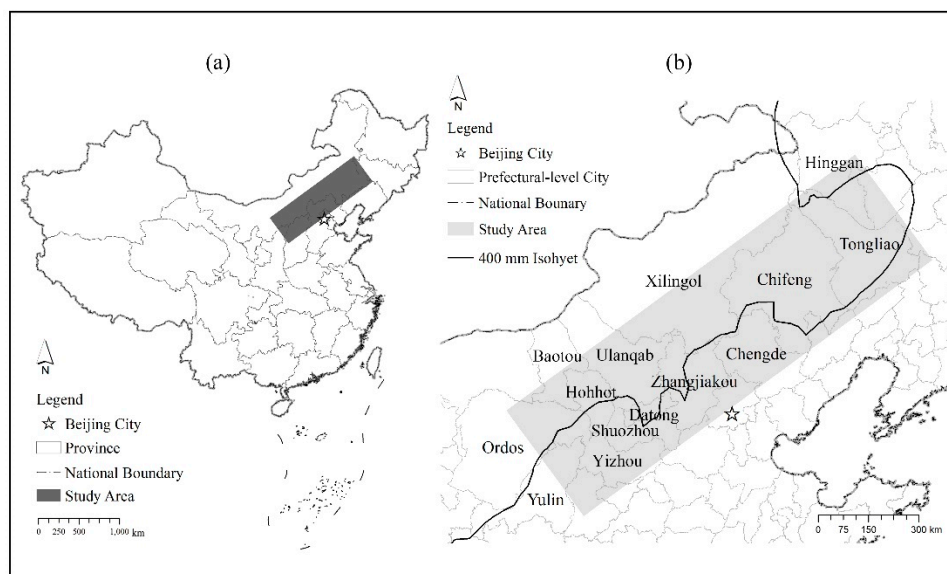


Figure 1. Location of the study area (a) within China and (b) at the local scale (Northern China) with annotation of the prefecture-level cities as well as the 400 mm mean annual precipitation isohyet considering the period 2006–2015.

2.2. Spatial Continuous Wavelet Transform

A wavelet transform can decompose signals over functions with varying window sizes. The window size adjusts to the frequency of the input signals [35], thus, it is well suited to signals with a wide range of frequencies [7,22]. The continuous wavelet transform (CWT) is efficient in detecting the dynamic trends and break points of continuous signals [7]. It can decompose signal vector ($f(t)$) by finite basis wavelet function ($\varphi(t)$) with a scale (a) and a shift (b) into wavelet coefficients (W_f), described as follows [36–38]:

$$W_f(a, t) = f(t)\varphi(t) = \frac{1}{\sqrt{a}} \int_{-\infty}^{+\infty} f(t)\varphi\left(\frac{t-b}{a}\right) dt \quad (1)$$

Subsequently, by replacing temporal signals with a geospatial element sequence ($S(x)$), the CWT is reformed into spatial continuous wavelet transform (SCWT), described as follows [7,30,37,38]:

$$SCWT(a, b) = \frac{1}{\sqrt{\alpha}} \int_0^{Lx} S(x)\varphi\left(\frac{x-b}{a}\right) dx \quad (2)$$

The SCWT can be used in spatial analysis, especially when decomposing the dynamic trends and mutation points from geospatial sequences [7,38]. In general, the coefficient modulus of the SCWT varies from 0 to 1. When SCWT is applied to boundary analysis, the higher coefficient modulus refers to a more rapid change of the input indicator, and the maximum value of the coefficient modulus is defined as the mutation point or break point of the spatial sequence. The Daubechies-3 (db3) wavelet filter (wavelet function shown in Figure 2a) was chosen as the mother wavelet. This is a compactly supported orthonormal wavelet with multiple resolutions, and has been widely used for mutation detection and trend analysis [39]. The db3 wavelet filter has been proved efficient in identifying the ecological boundary of the semi-arid or sub-humid transition zone in Northern China [30,31]. The scale factor is an inherent property of the wavelet filter. A small scale refers to a compressed wavelet and contains more information on rapidly changing details, whereas a larger scale refers to a stretched wavelet and provides more insights on slowly changing features [37,40]. The suitable scale of SCWT in this study was verified by plotting the variance curve of wavelet coefficients (Figure 2b), which illustrated the variance of wavelet coefficients of NDVI sequence at different scales. Figure 2b showed the inflection point and the maximum value of the variance curve as being detected at scale 3, which indicated that the most appropriate fitting scale of this input signal was scale 3 [41]. A calculation of the variances for different NDVI sequences in the study area showed that their variance curves of wavelet coefficients all shared the same pattern as shown in Figure 2b. Therefore, scale 3 was used to process the SCWT in this study. The SCWT was achieved using MATLAB R2016b software (The MathWorks, Inc., Natick, MA, USA).

For finite input signals, boundary effects occurred at the edge of the signals because the wavelet transform computing required values beyond the input signals, and therefore, may have reduced the accuracy of the results [42]. One common solution for the boundary effects is to extend the length of input signals [43]. The vegetation condition in the southeastern and northwestern side of the study area had different spatial patterns, and using the actual NDVI value beyond the study area may increase the uncertainty in the SCWT results. Hence, a simulation method was applied to extend the input NDVI sequences used to mitigate boundary effects. Each input NDVI sequence was extended from 40 elements to 60 elements using antisymmetric-padding (whole-point) extension method in MATLAB software. The extended elements were deleted after calculating the wavelet coefficients.

2.3. Spatial Pattern Analysis

The SCWT was accomplished using two different sets of input sequences, i.e., (i) the annual maximum NDVI and (ii) mean value of annual maximum NDVI covering the period 2006–2015. The absolute values of the wavelet coefficients were then calculated and categorized into three groups using the natural breaks method. After the wavelet coefficients modulus was found, analyses were performed to determine:

- (i) The mutation points of each NDVI spatial sequence. The mutation points, determined as the element with the highest wavelet coefficients modulus for each input signal, were located where each NDVI sequence changed most rapidly. The mean center of the mutation points of each year was calculated by using the Mean Center Tool of ArcGIS Spatial Analyst Toolbox.
- (ii) The spatial autocorrelation of all points with the wavelet coefficients modulus value. Global Moran's Index was used to measure the spatial autocorrelation based on the wavelet coefficients modulus value, which allowed us to investigate whether these coefficients were spatially clustered [44,45]. This index was calculated by using the Spatial Autocorrelation Tool of ArcGIS Spatial Statistics Toolbox.
- (iii) The kernel density of all points with the wavelet coefficients modulus value. Kernel density is an efficient and commonly-used method to link the location of a given set of points and their spatial attributes as well as to estimate the spatial probability distribution around these points [37,46]. The kernel density of all sampling points was calculated by using the Kernel Density Tool of the ArcGIS Spatial Analyst Toolbox and weighted by the wavelet coefficients modulus in order

to delineate the spatial aggregation of the wavelet coefficients [47]. The mean value of kernel density was used to classify the study area into two sub-regions.

- (iv) The frequency distribution of the sub-regions during 2006–2015. By overlaying the annual distribution of kernel density, the frequency distribution of the sub-regions was calculated and mapped using the ArcGIS 10.2 software.

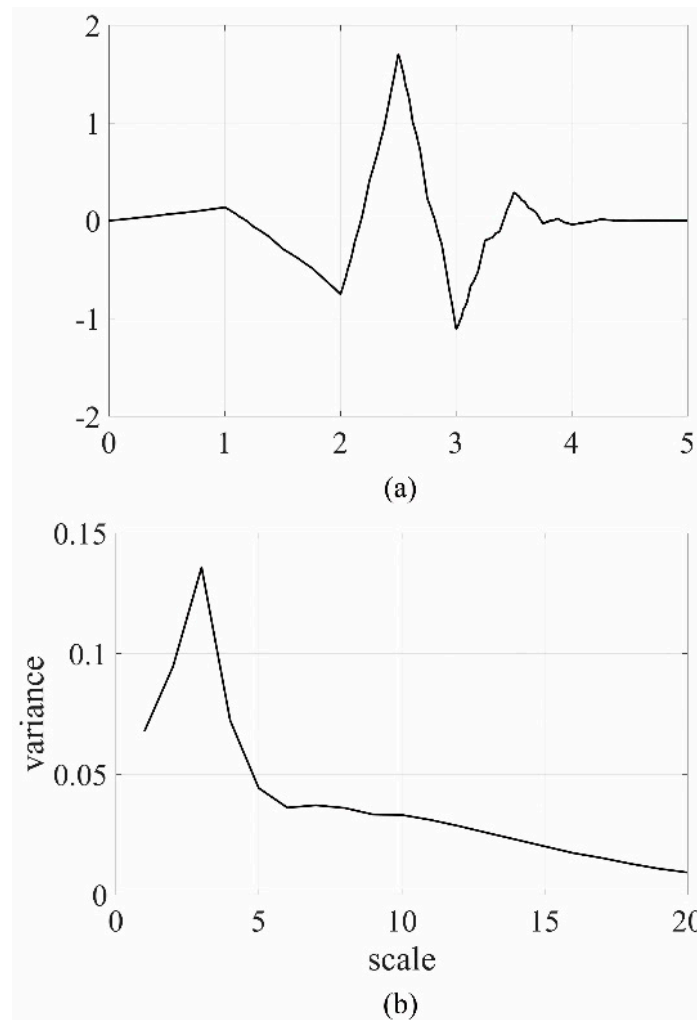


Figure 2. Wavelet filter and variance curve. (a) Wavelet function of the Daubechies-3 (db3) wavelet; (b) Variance curve of wavelet coefficients at different scales, using db3 filter.

3. Results and Discussions

3.1. Spatial Pattern of the APTZ

The distribution of mutation points of the NDVI sequences was in accordance with the spatial distribution of precipitation and landform features. As shown in Figure 3a, the mutation points of the mean NDVI value for the period 2006–2015 were mainly distributed along the southern part of the Greater Hinggan Range (Hinggan, Tongliao and Chifeng of Inner Mongolia), Bashang Plateau (Chifeng and Xilingol of Inner Mongolia, Chengde and Zhangjiakou of the Hebei Province) and Daqing Mountain (Ulanqab, Hohhot and Baotou of Inner Mongolia). Most of the mutation points were located in north of the 400 mm isohyet. The latter was consistent with the spatial distribution pattern of precipitation and landform features, and hence, revealed the general condition and extent of the APTZ in 2006–2015.

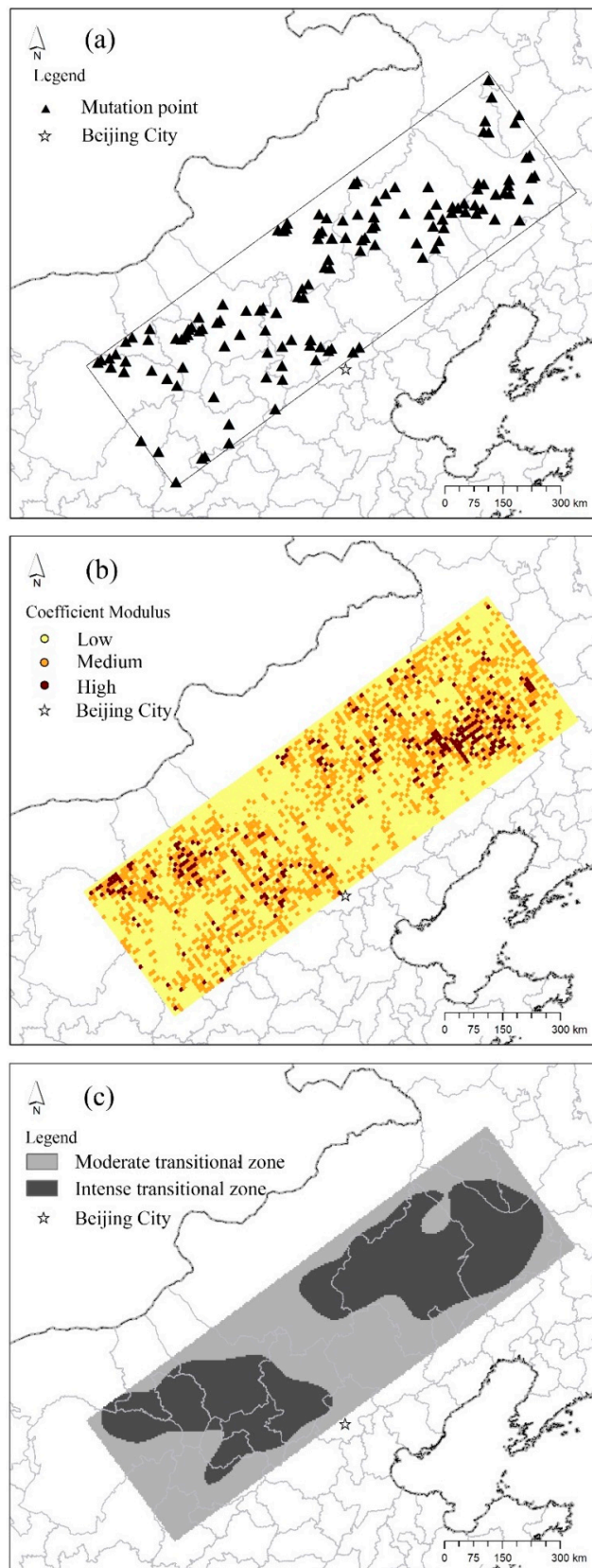


Figure 3. Spatial pattern of the wavelet coefficients modulus, using mean normalized difference vegetation index (NDVI) for the period 2006–2015. (a) Mutation points of each NDVI sequence; (b) classification of the wavelet coefficients module; (c) classification of the kernel density of the wavelet coefficients module.

The fluctuation of mean NDVI showed significant spatial autocorrelation. As shown in Figure 3b, the wavelet coefficients modulus had a tendency of spatial aggregation. The result of Global Moran's Index was 0.28 with a Z-score of 28.77, indicating the existence of a significant spatial autocorrelation in-between the wavelet coefficients modulus. That is to say, the fluctuation of mean NDVI appeared to have the characteristic of spatial aggregation. Hence, areas with drastic spatial change in vegetation coverage tend to be located in adjacent places, whereas areas with mild changes in vegetation coverage tend to be distributed continuously within adjacent areas.

According to the spatial fluctuation in the NDVI, the APTZ could be divided into two different types of zones based on the mean value of kernel density, i.e., (i) the intense transitional zone and (ii) the moderate transitional zone, as shown in Figure 3c. Areas with higher kernel density values than the mean value, were defined as the intense transitional zone of the APTZ; all the other areas were classified as the moderate transitional zone. Within the intense transitional zone, NDVI showed drastic fluctuation in a southeast-northwest direction, exhibiting a significant characteristic of spatial variation. Two intense transitional zones were identified in the study area, of which one (136,833 km²) was located in the northeast, mainly within the Xiliao River basin (Chifeng and Tongliao of Inner Mongolia). The other intense transitional zone (101,552 km²) was located in the southwest, within the region of the Tumochuan Plateau (Hohhot, Baotou and Ordos of Inner Mongolia), the south of the Daqing Mountains and the Sanggan River basin (Yizhou, Shuozhou and Datong of Shanxi Province). The moderate transitional zone of the APTZ comprised an area of approximately 264,715 km². Within the moderate transitional zone, NDVI showed gradual changes with few mutations and only mild fluctuation. As shown in Figure 3c, the moderate transitional zone was distributed continuously throughout the middle of the study area, including southern Xilingol in Inner Mongolia, northern Zhangjiakou and Chengde in Hebei Province, and in other places surrounding the intense transitional zone. According to the definition of an ecological boundary, the intense transitional zone, which showed a clear pattern of spatial variation in vegetation condition, was considered to be the crucial sub-region of the APTZ with greater importance for boundary study. Hence, the intense transitional zone was examined more closely, as described in subsequent sections.

3.2. Temporal Change of the Intense Transitional Zone

As shown in Figure 4, the core areas of the intense transitional zone remained stable during 2006–2015, while the fringe areas changed annually. Figure 5 showed the frequency distribution of the intense transitional zone during 2006–2015. In Figure 5, different grayscale intensities indicated different frequencies by which an area was identified as being part of the intense transitional zone over the 10-year studied period. More precisely, the darkest areas were identified as part of the intense transitional zone each year during 2006–2015, whereas the lightest areas were never identified as part of the intense transitional zone. As shown in Figure 5, the intense transitional zone had three highly stable core areas. These were located in the Xiliao River basin (area A), the Tumochuan Plateau (area B) and the Sanggan River basin (area C). In these areas, the vegetation condition showed significant spatial fluctuation, which underlined their crucial importance within the APTZ. In contrast, the area located in the northern part of Chengde and Zhangjiakou, also known as the Bashang Plateau (area D in Figure 5), was the largest area that remained in the moderate transitional zone during the study period. In this area, the vegetation condition declined gradually from the southeast to northwest. In all the other areas, the distribution of the intense transitional zone changed each year, and places nearby the core areas generally showed a higher frequency of being classified as parts of the intense transitional zone as compared to places far away from the core areas. This variation suggested that these regions had different sensitivity toward exterior factors affecting the spatial pattern of vegetation coverage, such as climatic variability and land use change.

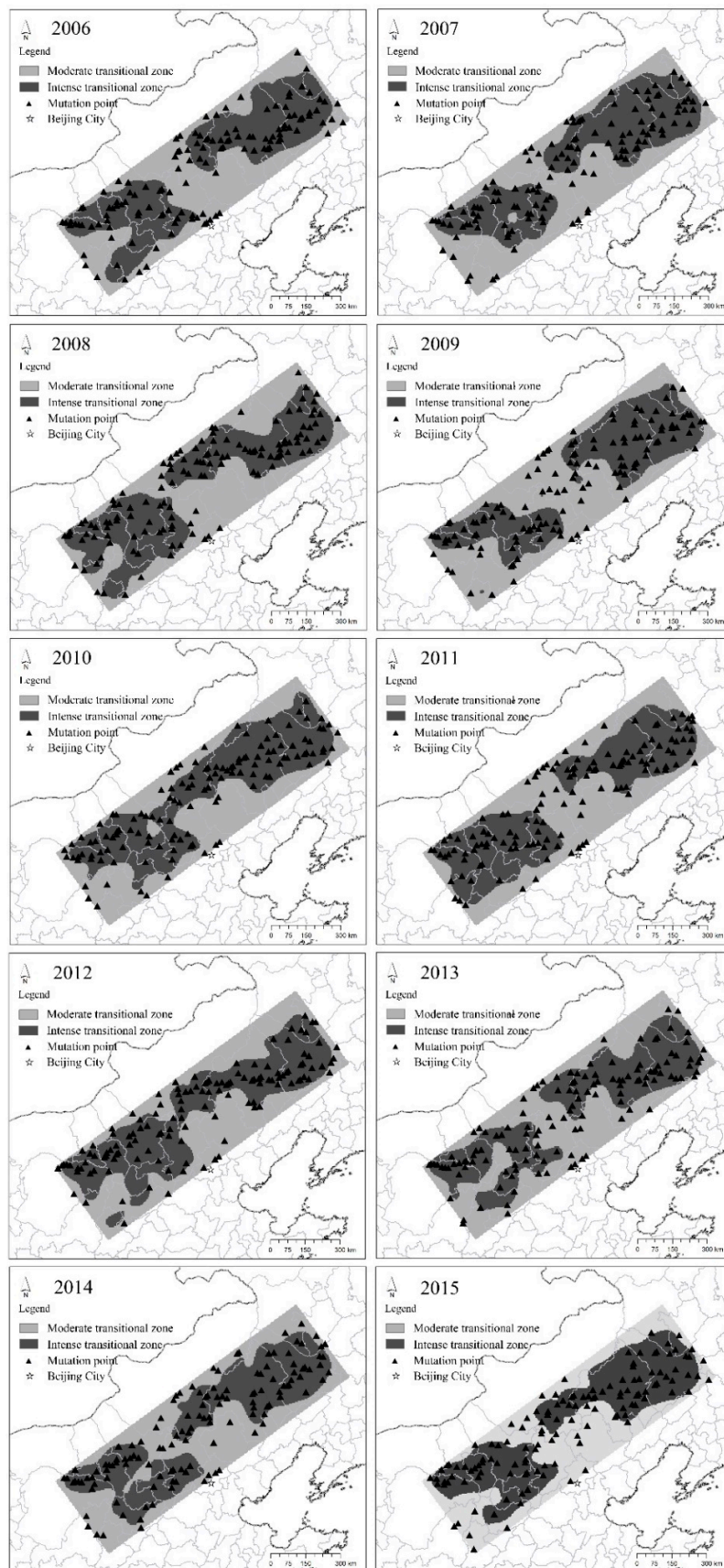


Figure 4. Temporal change of the agro-pastoral transitional zone (APTZ) and the spatial distribution of mutation points (2006–2015).

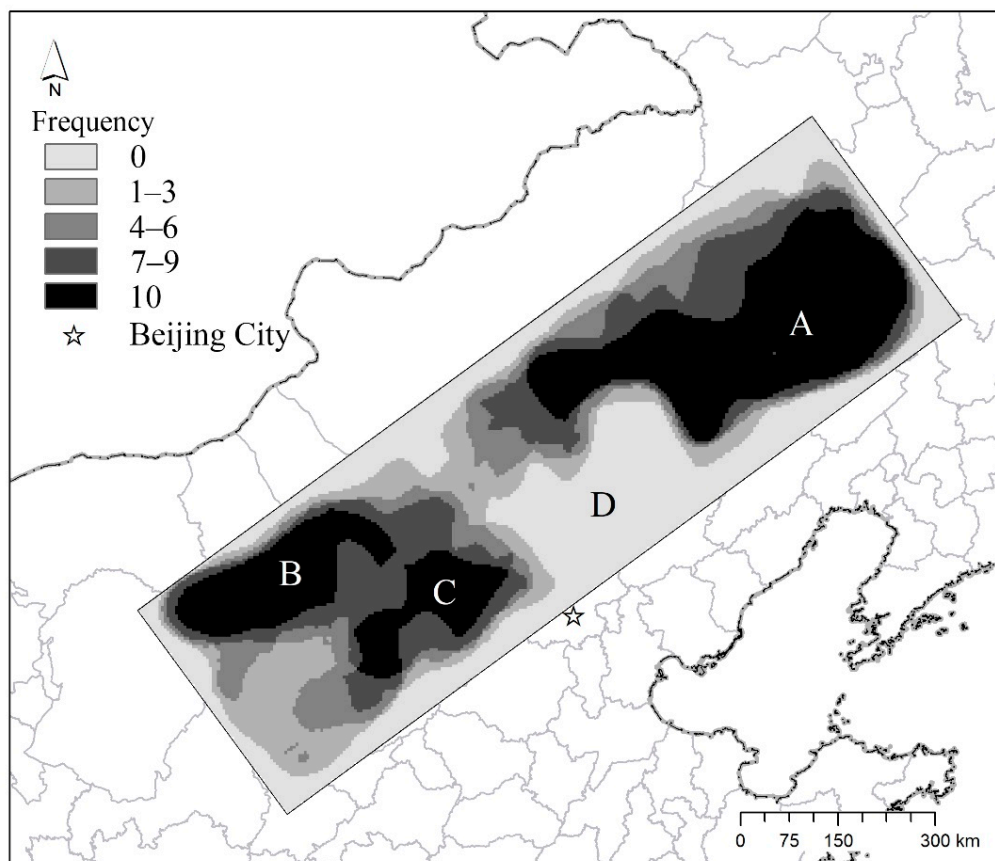


Figure 5. Frequency of identified intense transitional zone during 2006–2015. (Areas A, B and C were always identified as part of the intense transitional zone, while area D was never identified as part of the intense transitional zone).

Located along the northern edge of the East Asia Monsoon Region, the APTZ experiences remarkable inter-annual climatic variability (especially in precipitation), which has a great impact on vegetation growth and agricultural activities [26,48], and hence, on its turn influences the location and spatial characteristics of the APTZ [10,49]. By combining the annual precipitation and the mean center of the mutation points each year, the mean center of the APTZ was discovered to move toward the northwest in humid years and toward the southeast in dry years, along the vertical direction of the 400 mm isohyet of mean annual precipitation. Based on the annual precipitation data described in Section 2.1, the years 2006, 2007, 2009 and 2011 were identified as relative dry years that had negative anomalies on the average total precipitation, whereas the years 2008, 2010, 2012, 2013, 2014 and 2015 were identified as relatively humid years characterized by positive precipitation anomalies. The movement of the mean center each year and the associated precipitation condition are shown in Figure 6. It was clear that the location of the mean center was very close to the 400 mm mean annual precipitation isohyet corresponding to the year 2006–2015. This provides some clear evidence that the 400 mm isohyet can be considered as the central line of the APTZ [10,25,32]. Moreover, Figure 6 showed that in the year of 2009, which had the lowest total precipitation amount, the mean center was located in the most southeastern position, and in 2012, which was characterized by the highest total precipitation amount, the mean center was located in the most northwestern position, around 20 km away from the year of 2009. This movement reflects the typical vegetation response to precipitation variation. In years with less rainfall than average, the isohyet of annual precipitation generally moved toward the southeast, while in humid years the isohyet moved in the opposite direction (i.e., to the northwest). The result shows that the location of APTZ follows the variation of precipitation pattern, shifting along southeast-northwest direction.

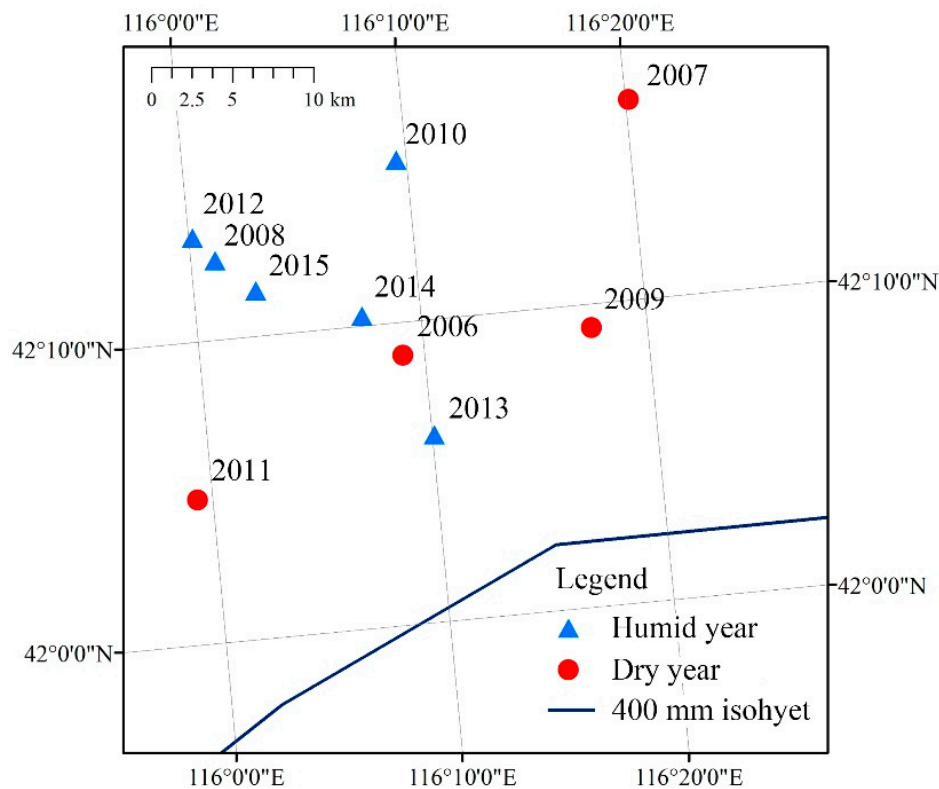


Figure 6. Temporal variation of the mean center of mutation points, compared with the 400 mm mean annual precipitation isohyet during 2006–2015.

3.3. Contrast with Traditional Identification of Agro-Pastoral Transitional Regions

To further examine the differences between the SCWT method used in this study and the traditional method (using the threshold of a climatic index), we chose mean annual precipitation during the period 2006–2015 as a contrast. Mean annual precipitation is the most commonly used climatic index in the APTZ studies, however, the threshold to delineate the boundary varies among studies [25]. For example, Wang et al. (1999) [50] suggested the APTZ should be defined as a region with mean annual precipitation of 250–500 mm, while Zhao et al. (2002) [51] defined this threshold as 300–450 mm. As shown in Figure 7, it was clear that the distribution of the intense transitional zone identified using SCWT followed the spatial pattern of mean annual precipitation amount, and was approximately similar to the range delineated by the 300–450 mm isohyet [51]. This was in particular the case in the southwestern part of the study area. In the northeastern part, the APTZ boundary, delineated by the above described precipitation threshold, was significantly larger than the intense transitional zone delineated by the SCWT. The major differences of the two results are shown in Figure 7 as regions A and B. Both of the two areas were within the APTZ identified using the precipitation threshold method, however, they were not within the intense transitional zone identified using the SCWT. Region A included the northern part of Chengde and Zhangjiakou as well as the southern part of Xilingol. As discussed in Section 3.2, this area showed a gradual spatial change in vegetation coverage, and was a traditional pasturing area with a typical grassland dominated landscape. Region B included the southeastern part of Ordos and the northern part of Yulin in the northeastern portion of the Ordos Plateau, and was also covered mainly by grassland. In this study, both of these areas were identified as part of the moderate transitional zone.

Furthermore, this comparison showed that the SCWT method provided a more precise characterization of the spatial changes in the ecological boundary than the traditional climatic threshold index method. The APTZ is a broad concept with multiple dimensions. From the view of an ecological boundary, it is important to emphasize the characteristics of discontinuity, fragmentation and

variation in landscape, land use and the spatial distribution of vegetation. The traditional definition has not given much attention to the interior spatial characteristics of the APTZ when delineating its general extent. The APTZ has been regarded as an integrated unit in traditional studies and the spatial heterogeneity within this unit has not drawn much attentions. In contrast, the SCWT method focuses on spatial features and can identify the areas in which vegetation exhibits most of the spatial variation. The SCWT method also avoids the subjectivity that arises in index selection and threshold definition. These advantages make the SCWT a better approach than traditional methods, and should preferentially be used to identify the APTZ in future studies. Since the APTZ is facing a stressful relationship between human well-being and environmental protection, uncovering the interior heterogeneity may provide a solid basis for future policy making in environmental management.

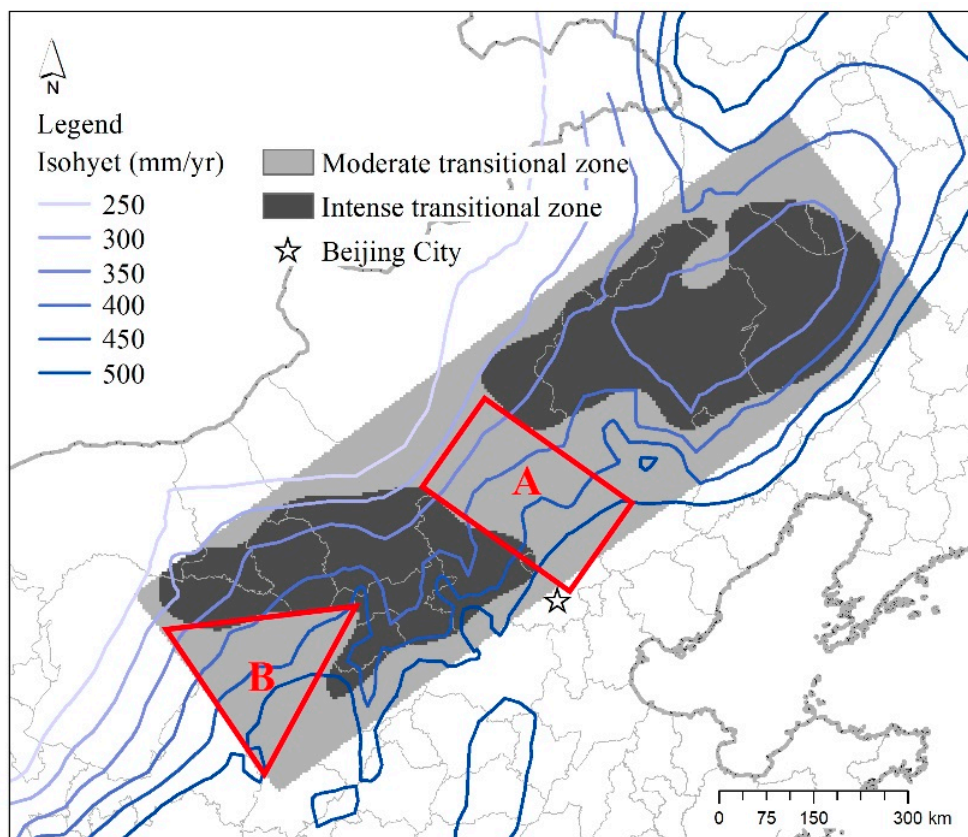


Figure 7. Comparison between the agro-pastoral transitional zone (APTZ) delineated using the threshold precipitation method and using the spatial continuous wavelet transform (SCWT) method with normalized difference vegetation index (NDVI). (Region A and B are representing the main differences between the two methods.).

3.4. Advantages, Limitations and Future Research Directions

As compared to the climate index and land use index, the NDVI showed significant advantages in characterizing the APTZ. The definition of APTZ based on climate indicators, such as annual precipitation and arid index, in fact refers to the potential distribution of the climatic transitional zone [10]. However, the actual condition of the transitional zone is not only influenced by climatic factors, but also by landform, soil resources, water resources, and human activity. On the other hand, the definition based on land use or other anthropogenic indices gives a higher importance to the impact that human beings and social-economic systems have on land resources. These indicators are easily influenced by market forces and land use policy, and therefore, may not be effective boundary detectors in the field of landscape ecology. Furthermore, climatic data are obtained from weather station measurements, which may have a negative impact on data availability and quality. Although

this type of data is typically characterized by high accuracy and temporal frequency, it is spatially discontinuous, and hence, significant errors may arise in the process of interpolating the data to cover large areas. Land use data, on the contrary, are an example of spatial data that have relatively lower accuracy and lower update frequency [52]. A shortage of both land use and climatic data generally exists in boundary studies. In contrast, NDVI data acquired by remote sensing are well suited for spatial analysis, and have advantages in terms of data accessibility and updating, as well as availability in multiple scales within continuous data sequences. In fact, it is a complex reflection of physical environmental conditions and human activities measured at a very high spatial-temporal frequency. Therefore, NDVI is an effective indicator in ecological boundary studies, and has been used in this study as the most useful vegetation indicator.

However, the SCWT method also has limitations. The accuracy of this method is highly dependent on spatial sampling. For complex geographical units, the sampling method must be adjusted to fit the spatial characteristics of the element being analyzed. For instance, in this study, the APTZ is an elongated area with a certain trend from northeast to southwest, so the indicator sequences can be sampled along lines that are perpendicular to the trend of the APTZ. For objects that expand outward from a central area, the indicator sequences can be sampled using radial transects with a common starting point [38]. If the sampling sequences were not set properly to fit the spatial structure of the study area, the SCWT method would not be effective. Moreover, the advantage of SCWT is its ability to detect mutation points and the rate of change along the studied spatial sequences. Thus, the selected indicator should reflect the most striking variations within the considered study area; otherwise, the analysis may lead to a large error in the identification result. For example, according to previous studies, the APTZ also covers areas of the Greater Hinggan Range, Loess Plateau and Hexi Corridor, which are mountain regions with complex landforms. Because vegetation in mountainous regions is largely influenced by landform, the complexity of landform may cause uncertainty in SCWT analysis. Therefore, to avoid the impact of complex landforms, this study focused on the central region of the APTZ characterized by a lower topographical complexity.

Future research should pay attention to the response of the APTZ to climate change. The APTZ is the most important ecological boundary in Northern China, and its structure and function are particularly sensitive to environmental variables. The response of the intense transitional zone to long term climate change effects, such as altered annual temperature and precipitation, should be examined by considering longer time series than those used in this study. Furthermore, vegetation dynamics under different climate change scenarios will lead to dynamic changes in boundary features and thus influence land use management. Consequently, identifying the potential future characteristics of the APTZ would be helpful in providing a scientific basis to policies that could influence this important area.

4. Conclusions

Given the current climate change, more attention has been given to ecological boundaries due to their sensitivity to external disturbances. The current techniques for identifying the APTZ are largely dependent on the subjective judgment of experts; thus, the accuracy of APTZ identification varies among studies. Additionally, the identification of ecological boundaries faces challenges in updating and incorporating dynamic research. The results showed that the SCWT method combined with NDVI data and kernel density estimation is much more reliable for identifying the spatial pattern within the APTZ, compared to the traditional methods based on climatic or land use thresholds. The approach also allowed the identification of sub-regions within the APTZ based on the spatial variation of vegetation condition. During 2006–2015, although the spatial pattern of vegetation variation changed annually and was highly influenced by exterior factors, some areas appeared to be stable, and others were more sensitive to environmental changes. This heterogeneity within the APTZ should be taken into consideration in future land use management.

Author Contributions: Conceptualization, Y.H., J.P., J.M., Z.Z. and Y.L.; data curation, Y.N.; formal analysis, Y.N.; funding acquisition, J.P.; investigation, Y.N. and Q.M.; methodology, Y.H. and Z.Z.; project administration, J.P.; resources, J.P.; software, Y.N.; supervision, J.P.; validation, Q.M.; visualization, Y.N. and Q.M.; writing—original draft, Y.N. and J.P.; writing—review and editing, Y.N., J.P., J.M., Z.Z. and Y.L.

Funding: This research was funded by the National Key R&D Program of China (No.2017YFA0604704) and the 111 Project (B14001).

Conflicts of Interest: The authors declare no conflict of interest. The founding sponsors had no role in the design of the study; in the collection, analyses, or interpretation of data; in the writing of the manuscript, and in the decision to publish the results.

References

- Caracciolo, D.; Noto, L.; Istanbuluoglu, E.; Fatichi, S.; Zhou, X. Climate change and Ecotone boundaries: Insights from a cellular automata ecohydrology model in a Mediterranean catchment with topography controlled vegetation patterns. *Adv. Water Resour.* **2014**, *73*, 159–175. [[CrossRef](#)]
- Strayer, D.; Power, M.; Fagan, W.; Pickett, S.; Belnap, J. A classification of ecological boundaries. *Bioscience* **2003**, *53*, 723–729. [[CrossRef](#)]
- Fagan, W.; Fortin, M.; Soykan, C. Integrating edge detection and dynamic modeling in quantitative analyses of ecological boundaries. *Bioscience* **2003**, *53*, 730–738. [[CrossRef](#)]
- Fortin, M.; Olson, R.; Ferson, S.; Iverson, L.; Hunsaker, C.; Edwards, G.; Levine, D.; Butera, K.; Klemas, V. Issues related to the detection of boundaries. *Landsc. Ecol.* **2000**, *15*, 453–466. [[CrossRef](#)]
- Jacquez, G.; Maruca, S.; Fortin, M. From fields to objects: A review of geographic boundary analysis. *J. Geogr. Syst.* **2000**, *2*, 221–241. [[CrossRef](#)]
- Risser, P. The status of the science examining ecotones: A dynamic aspect of landscape is the area of steep gradients between more homogeneous vegetation associations. *Bioscience* **1995**, *45*, 318–325. [[CrossRef](#)]
- Li, S.; Yang, Z.; Gao, Y. Scale-Dependent Spatial Relationships between NDVI and Abiotic Factors. *J. Resour. Ecol.* **2010**, *1*, 361–367. [[CrossRef](#)]
- Zhao, Z.; Liu, J.; Peng, J.; Li, S.; Wang, Y. Non-linear features and complexity patterns of vegetation dynamics in the transition zone of North China. *Ecol. Indic.* **2015**, *49*, 237–246. [[CrossRef](#)]
- Zhao, Z.; Gao, J.; Wang, Y.; Liu, J.; Li, S. Exploring spatially variable relationships between NDVI and climatic factors in a transition zone using geographically weighted regression. *Theor. Appl. Climatol.* **2015**, *120*, 507–519. [[CrossRef](#)]
- Ye, Y.; Fang, X. Boundary shift of potential suitable agricultural area in farming-grazing transitional zone in Northeastern China under background of climate change during 20th century. *Chin. Geogr. Sci.* **2013**, *23*, 655–665. [[CrossRef](#)]
- Cao, Q.; Yu, D.; Georgescu, M.; Han, Z.; Wu, J. Impacts of land use and land cover change on regional climate: A case study in the agro-pastoral transitional zone of China. *Environ. Res. Lett.* **2015**, *10*, 124025. [[CrossRef](#)]
- Yu, L. Agro-pastoralism under climate change: Institutions and local climate adaptations in northern China. *Land Use Policy* **2016**, *58*, 173–182. [[CrossRef](#)]
- Huang, D.; Wang, K.; Wu, W. Dynamics of soil physical and chemical properties and vegetation succession characteristics during grassland desertification under sheep grazing in an agro-pastoral transition zone in northern China. *J. Arid Environ.* **2007**, *70*, 120–136. [[CrossRef](#)]
- Qi, Y.; Chang, Q.; Jia, K.; Liu, M.; Liu, J.; Chen, T. Temporal-spatial variability of desertification in an agro-pastoral transitional zone of northern Shaanxi Province, China. *Catena* **2012**, *88*, 37–45. [[CrossRef](#)]
- Van der Maarel, E. On the establishment of plant community boundaries. *Ber. Deutsch. Bot. Ges.* **1976**, *89*, 415–443. [[CrossRef](#)]
- Fortin, M. Effects of quadrat size and data measurement on the detection of boundaries. *J. Veg. Sci.* **1999**, *10*, 43–50. [[CrossRef](#)]
- He, R.; Yang, J.; Song, X. Quantifying the impact of different ways to delimit study areas on the assessment of species diversity of an urban forest. *Forests* **2016**, *7*, 42. [[CrossRef](#)]
- Fortin, M.; Drapeau, P. Delineation of ecological boundaries: Comparison of approaches and significance tests. *Oikos* **1995**, *72*, 323–332. [[CrossRef](#)]
- Davis, D.; Gagne, S. Boundaries in ground beetle (Coleoptera: Carabidae) and environmental variables at the edges of forest patches with residential developments. *PEERJ* **2018**, *6*, e4226. [[CrossRef](#)]

20. Keitt, T.; Urban, D. Scale-specific inference using wavelets. *Ecology* **2005**, *86*, 2497–2504. [[CrossRef](#)]
21. Zhang, L.; Bao, P. Edge detection by scale multiplication in wavelet domain. *Pattern Recogn. Lett.* **2002**, *23*, 1771–1784. [[CrossRef](#)]
22. Cazelles, B.; Chavez, M.; Berteaux, D.; Menard, F.; Vik, J.; Jenouvrier, S.; Stenseth, N.C. Wavelet analysis of ecological time series. *Oecologia* **2008**, *156*, 287–304. [[CrossRef](#)] [[PubMed](#)]
23. Csillag, F.; Kabos, S. Wavelets, boundaries, and the spatial analysis of landscape pattern. *Écoscience* **2002**, *9*, 177–190. [[CrossRef](#)]
24. James, P.; Fleming, R.; Fortin, M. Identifying significant scale-specific spatial boundaries using wavelets and null models: Spruce budworm defoliation in Ontario, Canada as a case study. *Landsc. Ecol.* **2010**, *25*, 873–887. [[CrossRef](#)]
25. Liu, J.; Gao, J.; Lv, S.; Han, Y.; Nie, Y. Shifting farming-pastoral ecotone in China under climate and land use changes. *J. Arid Environ.* **2011**, *75*, 298–308. [[CrossRef](#)]
26. Gong, D.; Shi, P.; Wang, J. Daily precipitation changes in the semi-arid region over northern China. *J. Arid Environ.* **2004**, *59*, 771–784. [[CrossRef](#)]
27. Dong, J.; Liu, J.; Yan, H.; Tao, F.; Kuang, W. Spatio-temporal pattern and rationality of land reclamation and cropland abandonment in mid-eastern Inner Mongolia of China in 1990–2005. *Environ. Monit. Assess.* **2011**, *179*, 137–153. [[CrossRef](#)] [[PubMed](#)]
28. Qiao, J.; Yu, D.; Wu, J. How do climatic and management factors affect agricultural ecosystem services? A case study in the agro-pastoral transitional zone of northern China. *Sci. Total Environ.* **2018**, *613*, 314–323. [[CrossRef](#)] [[PubMed](#)]
29. Wang, X.; Li, Y.; Chen, Y.; Lian, J.; Luo, Y.; Niu, Y.; Gong, X.; Yu, P. Temporal and spatial variation of extreme temperatures in an agro-pastoral ecotone of northern China from 1960 to 2016. *Sci. Rep.* **2018**, *8*, 8787. [[CrossRef](#)] [[PubMed](#)]
30. Li, S.; Zhao, Z.; Gao, J. Identifying eco-geographical boundary using spatial wavelet transform. *Acta Ecol. Sin.* **2008**, *28*, 4313–4322. (In Chinese)
31. Zhao, Z. Vegetation Dynamics and Climate Factors in the Eco-Geographical Transition Zone and Surrounding Areas of North China. Ph.D. Thesis, Peking University, Beijing, China, 2015. (In Chinese)
32. Shi, W.; Liu, Y.; Shi, X. Development of quantitative methods for detecting climate contributions to boundary shifts in farming-pastoral ecotone of northern China. *J. Geogr. Sci.* **2017**, *27*, 1059–1071. [[CrossRef](#)]
33. Myneni, R.; Keeling, C.; Tucker, C.; Asrar, G.; Nemani, R. Increased plant growth in the northern high latitudes from 1981 to 1991. *Nature* **1997**, *386*, 698–702. [[CrossRef](#)]
34. Chen, X.; Hu, B.; Yu, R. Spatial and temporal variation of phenological growing season and climate change impacts in temperate eastern China. *Glob. Chang. Biol.* **2005**, *11*, 1118–1130. [[CrossRef](#)]
35. Lau, K.; Weng, H. Climate signal detection using wavelet transform: How to make a time series sing. *Bull. Am. Meteorol. Soc.* **1995**, *76*, 2391–2402. [[CrossRef](#)]
36. Martínez, B.; Gilbert, M. Vegetation dynamics from NDVI time series analysis using the wavelet transform. *Remote Sens. Environ.* **2009**, *113*, 1823–1842. [[CrossRef](#)]
37. Peng, J.; Zhao, S.; Liu, Y.; Tian, L. Identifying the urban-rural fringe using wavelet transform and kernel density estimation: A case study in Beijing City, China. *Environ. Model. Softw.* **2016**, *83*, 286–302. [[CrossRef](#)]
38. Peng, J.; Hu, Y.; Liu, Y.; Ma, J.; Zhao, S. A new approach for urban-rural fringe identification: Integrating impervious surface area and spatial continuous wavelet transform. *Landsc. Urban Plan.* **2018**, *175*, 72–79. [[CrossRef](#)]
39. Bing, L.; Shao, Q.; Liu, J. Runoff characteristics in flood and dry seasons based on wavelet analysis in the source regions of the Yangtze and Yellow rivers. *J. Geogr. Sci.* **2012**, *22*, 261–272. [[CrossRef](#)]
40. Nakken, M. Wavelet analysis of rainfall-runoff variability isolating climatic from anthropogenic patterns. *Environ. Model. Softw.* **1999**, *14*, 283–295. [[CrossRef](#)]
41. Mallat, S. *A Wavelet Tour of Signal Processing: The Sparse Way*, 3rd ed.; Academic Press: New York, NY, USA, 2008; ISBN-13: 978-0123743701.
42. Queiroz, R. Subband processing of finite length signals without border distortions. *Acoust. Speech Signal Process.* **1992**, *4*, 613–616. [[CrossRef](#)]
43. Su, H.; Liu, Q.; Li, J. Boundary effects reduction in wavelet transform for time-frequency analysis. *WSEAS Trans. Signal Process.* **2012**, *8*, 169–179.
44. Moran, P. The interpretation of statistical maps. *J. R. Stat. Soc. B* **1948**, *10*, 243–251. [[CrossRef](#)]

45. Getis, A.; Ord, K. The Analysis of Spatial Association by Use of Distance Statistics. *Geogr. Anal.* **1992**, *24*, 189–206. [[CrossRef](#)]
46. Brundson, C. Estimating probability surfaces for geographical point data: An adaptive kernel algorithm. *Comput. Geosci.* **1995**, *21*, 877–894. [[CrossRef](#)]
47. Silverman, B. *Density Estimation for Statistics and Data Analysis*; Chapman and Hall: New York, NY, USA, 1986; ISBN-13: 978-0412246203.
48. Lau, K.; Yang, G.; Shen, S. Seasonal and intraseasonal climatology of summer monsoon rainfall over East-Asia. *Mon. Weather Rev.* **1988**, *116*, 18–37. [[CrossRef](#)]
49. Cadenasso, M.; Pickett, S.; Weathers, K.; Jones, C. A framework for a theory of ecological boundaries. *Bioscience* **2003**, *53*, 750–758. [[CrossRef](#)]
50. Wang, J.; Xu, X.; Liu, P. Landuse and land carrying capacity in ecotone between agriculture and animal husbandry in Northern China. *Resour. Sci.* **1999**, *21*, 19–24. (In Chinese)
51. Zhao, H.; Zhao, X.; Zhang, T.; Zhou, R. Boundary line on agro-pasture zigzag zone in North China and its problems on eco-environment. *Adv. Earth Sci.* **2002**, *17*, 739–747. (In Chinese)
52. Yu, W.; Zhou, W.; Qian, Y.; Yan, J. A new approach for land cover classification and change analysis: Intergrating backdating and an object-based method. *Remote Sens. Environ.* **2016**, *177*, 37–47. [[CrossRef](#)]



© 2018 by the authors. Licensee MDPI, Basel, Switzerland. This article is an open access article distributed under the terms and conditions of the Creative Commons Attribution (CC BY) license (<http://creativecommons.org/licenses/by/4.0/>).